Tellus (1992), *44A*, 18–32

On the normal modes of Laplace's tidal equations for zonal wavenumber zero

By H. L. TANAKA[1], *Geophysical Institute, University of Alaska Fairbanks, Fairbanks, Alaska 99775-0800, USA* and AKIRA KASAHARA, *National Center for Atmospheric Research*, Boulder, Colorado 80307, USA*

(Manuscript received 1 February 1991; in final form 19 June 1991)

ABSTRACT

Normal modes of Laplace's tidal equations, referred to as Hough harmonics, are complete for zonal wavenumber $m > 0$ so that the longitudinal and meridional velocity components and the geopotential can be represented as a series of Hough harmonics. However, Hough harmonics corresponding to $m = 0$ are incomplete in that the second kind normal modes have all zero frequencies. To fill the need for orthonormal basis functions, Kasahara and Shigehisa have constructed two different sets of the rotational modes of Laplace's tidal equations for $m = 0$, referred to as the K-modes and the S-modes, respectively. In this study, we compared the characteristic differences between the K- and S-modes in their energy ratio and structures. The zonal-mean components of atmospheric data from the FGGE IIIb reanalysis are projected onto the K- and S-modes separately, in addition to the gravity modes. We showed that the K-mode representation captures the majority of observed zonal energy with a few terms, whereas the S-mode representation requires many terms. The K-mode series converges faster than the S-mode series, especially for small vertical-scale components in the observed zonal fields. The differences between the energy spectra projected upon the K- and S-modes are discussed along with the consideration of the merits of each set as expansion functions for the zonal atmospheric motions.

1. Introduction

Small-amplitude motions of a thin, uniform layer of fluid over a rotating sphere are governed by Laplace's tidal equations. Historically, eigensolutions of Laplace's tidal equations have been used to solve atmospheric tidal problems (Chapman and Lindzen 1970). In recent years, the eigensolutions of free oscillations described by Laplace's tidal equations, referred to as the normal modes, have been applied to the problem of data initialization (Errico 1989), to the numerical integrations of the global shallow-water equations (Kasahara 1977; Salby et al., 1990), and to the diagnosis of global atmospheric energetics (Kasahara and Puri 1981; Tanaka 1985; Tanaka et al., 1986).

The characteristics of the normal modes of Laplace's tidal equations have been discussed, for example, by Longuet-Higgins (1968). In general, there are two kinds of solutions. One, called oscillations of the first kind, consists of the gravity-inertia waves which propagate eastwards and westwards. The other, called oscillations of the second kind, consists of the westward propagating rotational waves, often referred to as Rossby-Haurwitz waves. For nonzonal motions with zonal wavenumber greater than zero, Hough harmonics are discrete and orthogonal. However, the case of zonal wavenumber zero is special in that the frequencies of gravity modes (first kind) appear as pairs of positive and negative values of the same magnitudes, and the frequencies of the rotational modes (second kind) are all zero. Therefore, the rotational modes corresponding to zonal wavenumber $m = 0$ are not unique. It is necessary

[1] Present affiliation: Institute of Geoscience, University of Tsukuba, Ibaraki 305, Japan.

* The National Center for Atmospheric Research is sponsored by the National Science Foundation.

to have a complete set of the eigenfunctions of zonal rotational motions in order to expand atmospheric data in terms of a series of Hough harmonics.

In the case of $m = 0$, Laplace's tidal equations for the rotational motions degenerate to the linear balance equation for zonal flows on the sphere. Since the balance equation is a generalized form of the geostrophic equation, we shall refer to the Hough harmonics of the rotational modes for $m = 0$ as geostrophic modes. Kasahara (1978) constructed a set of meridional functions corresponding to the geostrophic modes by a series of Legendre polynomials, and applied the Gram-Schmidt procedure to obtain an orthonormal set. These will be referred to as the K-modes. Tribbia (1979) adopted a similar procedure to construct geostrophic modes for his study of data initialization using the equatorial beta-plane shallow-water model.

For nonzonal wavenumbers, the normal modes of linearized equatorial beta-plane shallow-water system form a complete and orthogonal set (Matsuno 1966). The eigenfrequencies of the rotational modes vanish in the case of zonal wavenumber zero and, therefore, the proof of the orthogonality of eigenfunctions fails in much the same way as the case of Laplace's tidal equations. To fulfill the need of orthogonal expansion functions for the rotational motions, Silva Dias and Schubert (1979) constructed an orthogonal set of geostrophic modes by taking the limit of the eigenfunctions of the rotational modes as the zonal wavenumber approaches to zero, and applying L'Hôpital's rule to derive the eigenfunctions.

Shigehisa (1983) obtained the geostrophic modes of Laplace's tidal equations as the limit of rotational modes for $m \to 0$. This is essentially the same as Silva Dias and Schubert's approach for the case of the equatorial beta-plane model. However, unlike the equatorial beta-plane model, in which the zonal wavenumber is a real number, the zonal wavenumber m for a spherical domain becomes an integer. The limit of eigensolutions of the rotational modes is calculated by considering m to be a continuous parameter and the ratio between m and the corresponding eigenfrequency σ to be finite. The latter condition ensures the phase speed $c = \sigma/m$ to be continuous with respect to m. By this approach, Shigehisa obtained orthogonal geostrophic modes, which are referred to as the S-modes. They have similar characteristics with the rotational modes for $m > 0$. In a software package developed by Swarztrauber and Kasahara (1985), the S-modes are calculated instead of the K-modes.

Since two sets of the geostrophic modes have been proposed, it is meaningful to examine the difference in the properties of the K- and S-modes. We are particularly interested in the spectral characteristics of the observed zonal mean atmospheric states in terms of the two different sets of the geostrophic modes. The atmospheric zonal states are projected onto the two sets of geostrophic modes to complement the normal-mode energetic studies of Tanaka (1985), Tanaka and Kung (1988), and Tanaka and Sun (1990). For that purpose, we used the reanalyzed Level IIIb datasets from the First GARP (Global Atmospheric Research Program) Global Experiment (FGGE) for the Special Observing Period I (SOP-I) provided by the Geophysical Fluid Dynamics Laboratory (GFDL). The differences in the meridional energy spectra are examined to assess the merits of the two sets of geostrophic modes.

2. Normal modes for zonal wavenumber zero

We describe briefly the derivation of the normal modes for wavenumber $m = 0$ following Swarztrauber and Kasahara (1985). A system of linearized shallow water equations in spherical coordinates of longitude λ and latitude θ for a resting basic state may be reduced to the following eigenvalue problem:

$$LH_m = i\sigma H_m. \tag{1}$$

where

$$L = \begin{pmatrix} 0 & -\sin\theta & \dfrac{\alpha}{\cos\theta}\dfrac{\partial}{\partial\lambda} \\ \sin\theta & 0 & \alpha\dfrac{\partial}{\partial\theta} \\ \dfrac{\alpha}{\cos\theta}\dfrac{\partial}{\partial\lambda} & \dfrac{\alpha}{\cos\theta}\dfrac{\partial(\ )\cos\theta}{\partial\theta} & 0 \end{pmatrix}, \tag{2}$$

and σ is the dimensionless eigenfrequency, scaled

by 2Ω. The parameter $\alpha = \sqrt{gh}/(2\Omega a)$ is a single dimensionless constant that characterizes the nature of shallow water flows. The eigensolutions $H_m(\lambda, \theta)$ of (1) are referred to as Hough harmonics of wavenumber m and are defined by a product of Hough vector functions $(U, -iV, Z)^T$ and $e^{im\lambda}$. The components U, V, and Z represent the dimensionless longitudinal and meridional velocity, scaled by $\sqrt{gh}$, and the dimensionless geopotential, scaled by gh, respectively. Here, the symbols are the earth's radius a, the earth's gravity g, the angular speed of the earth's rotation Ω, and the equivalent height h.

In order to determine the Hough vector functions, we assume a series solution for $H_m(\lambda, \theta)$, in terms of spherical vector harmonics $y^m_{n,1}$, $y^m_{n,2}$, and $y^m_{n,3}$ with expansion coefficients A^m_n, B^m_n, and C^m_n:

$$H_m(\lambda, \theta) = \sum_{n=0}^{\infty} (iA^m_n y^m_{n,1} + B^m_n y^m_{n,2} - C^m_n y^m_{n,3}). \quad (3)$$

Refer to Swarztrauber and Kasahara (1985) for the description of the spherical vector harmonics which form a complete set of vector functions defined on the sphere under a suitable inner product. Substituting (3) into (1) and collecting the expansion coefficients of the same spherical vector harmonics, we can obtain relations to be satisfied for the expansion coefficients.

We shall discuss only the solutions of the second kind for $m = 0$, and the reference to superscripts m will be eliminated in the following presentation. The frequencies of the rotational modes are identically zero for $m = 0$. This results in $V = 0$, a strictly zonal flow, and $A_n = 0$ in (3). The required equation to be satisfied by the rotational modes is a geostrophic balance between U and Z. We thus refer to the modes as geostrophic modes. The meridional index may be assigned as $l_R = 0, 1, 2, \ldots$ by the analogy of the nonzonal rotational modes. After some manipulations, the required geostrophic relation for the coefficients becomes

$$r_n C_n + p_n B_{n-1} + p_{n+1} B_{n+1} = 0, \quad (4)$$

where

$$r_n = \alpha \sqrt{n(n+1)}, \quad (5)$$

$$p_n = \sqrt{\frac{(n-1)(n+1)}{(2n-1)(2n+1)}}. \quad (6)$$

Expansion coefficients B_n and C_n are related to U and Z fields, respectively.

Kasahara (1978) observed that any combination of U and Z satisfying the geostrophic relation (4) can be a basis function of the geostrophic modes. One such a set of U and Z is constructed by specifying

$$\left.\begin{aligned} &B_n = 1, && \text{for} \quad n = l_R \\ &B_n = 0, && \text{for all other } n \end{aligned}\right\}, \quad (7)$$

where $l_R = 1, 2, 3, \ldots$. We then calculate C_n from (4) as

$$\left.\begin{aligned} &C_{n-1} = -p_n / r_{n-1}, \\ &\quad \text{and} \quad C_{n+1} = -p_{n+1}/r_{n+1}, \\ &\quad \text{for} \quad n = l_R \\ &C_n = 0, \quad \text{for all other } n \end{aligned}\right\}. \quad (8)$$

Once B_n and C_n are determined, the Hough harmonics are evaluated as a series of (3). The mode corresponding to $l_R = 0$ is that both U and V are identically zero and Z is a nonzero constant. The resulting modes are not orthogonal, so they are orthogonalized using the Gram-Schmidt process. Hereafter, we refer to these as the K-modes.

Shigehisa (1983) proposed an alternative derivation of geostrophic modes by assuming that the following limits exist: $\sigma/m \to c$ and $A_n/m \to \tilde{A}_n$ as $m \to 0$. The quantity c has the analogy of dimensionless phase speed. In this derivation, the relation to be satisfied for the geostrophic modes can be reduced for B_n by eliminating $\hat{A}_n$ and C_n:

$$d_{n-1} e_{n-1} \hat{B}_{n-2} + [n(n+1) + e^2_{n-1} + d^2_{n+1} + c^{-1}] \times \hat{B}_n + d_{n+1} e_{n+1} \hat{B}_{n+2} = 0, \quad (9)$$

where

$$d_n = \frac{(n-1)}{\alpha \sqrt{(2n-1)(2n+1)}}, \quad (10)$$

$$e_n = \frac{(n+2)}{\alpha \sqrt{(2n+1)(2n+3)}}, \quad (11)$$

and we have replaced B_n by $\hat{B}_n$ as

$$B_n = \sqrt{n(n+1)}\, \hat{B}_n. \quad (12)$$

The balance condition (4) is also expressed by $\hat{B}_n$ as

$$C_n = -d_n \hat{B}_{n-1} - e_n \hat{B}_{n+1}. \quad (13)$$

Equation (9) can be solved as eigenvalue problems of two independent tridiagonal systems for $\hat{B}_n$ with the eigenvalue c^{-1} from which the normal modes are constructed. One system gives symmetric solutions with odd subscripts $n = -1, 1, 3, \ldots$. The other gives antisymmetric solutions with even subscripts $n = 2, 4, 6, \ldots$. All eigenvalues c^{-1} are found to be negative except one for $n = -1$, which is positive. Therefore, we designate the lowest symmetric mode to be $l_R = -1$, as done by Shigehisa (1983). This mode has a property analogous to the eastward propagating Kelvin mode. Hereafter, we refer to these geostrophic modes as the S-modes. The proof of the orthogonality of S-modes has been discussed by Shigehisa and Swarztrauber and Kasahara (1985).

For each Hough vector function so obtained,

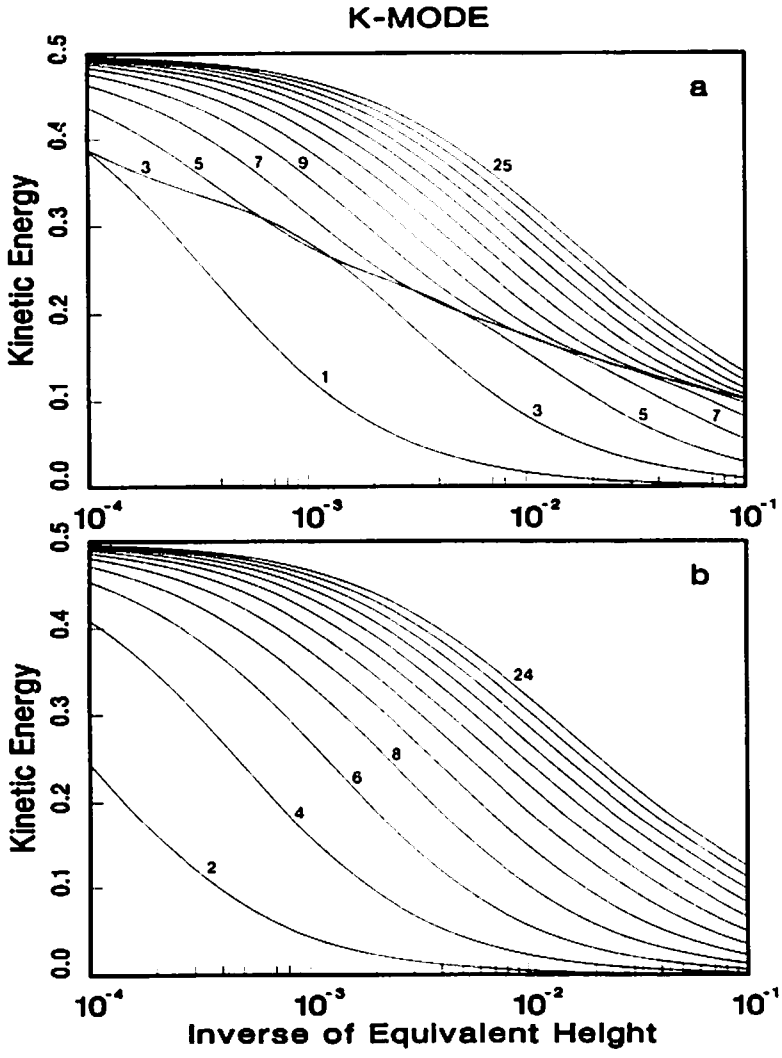

Fig. 1. Normalized kinetic energy of the K-modes as functions of equivalent height h_k. (a) Symmetric modes with odd meridional indices. $l_R = 1, 3, 5, \ldots$, and (b) antisymmetric modes with even indices. $l_R = 2, 4, 6, \ldots$.

we define the components of kinetic energy and potential energy by

$$\begin{pmatrix} K_u \\ K_v \\ P \end{pmatrix} = \frac{1}{2}\int_{-\pi/2}^{\pi/2} \begin{pmatrix} U^2 \\ V^2 \\ Z^2 \end{pmatrix} \cos\theta \, d\theta. \qquad (14)$$

We use the same normalization as in Kasahara (1976), thus $K_u + K_v + P = 0.5$, and $K_v = 0$ for the geostrophic modes.

Figs. 1 and 2 describe the normalized kinetic energy levels for the K-modes and S-modes, respectively, as functions of the inverse of equivalent height h. The solid lines of Fig. 1 for the K-modes indicate a tendency of increasing kinetic energy for increasing meridional index l_R. The energy level approaches 0.5 faster for the external mode at $h = 10^4$ m than the rest of internal modes. This implies that the variance of U dominates over that of Z in the modal structures. As h^{-1} increases, the kinetic energy level decreases and eventually

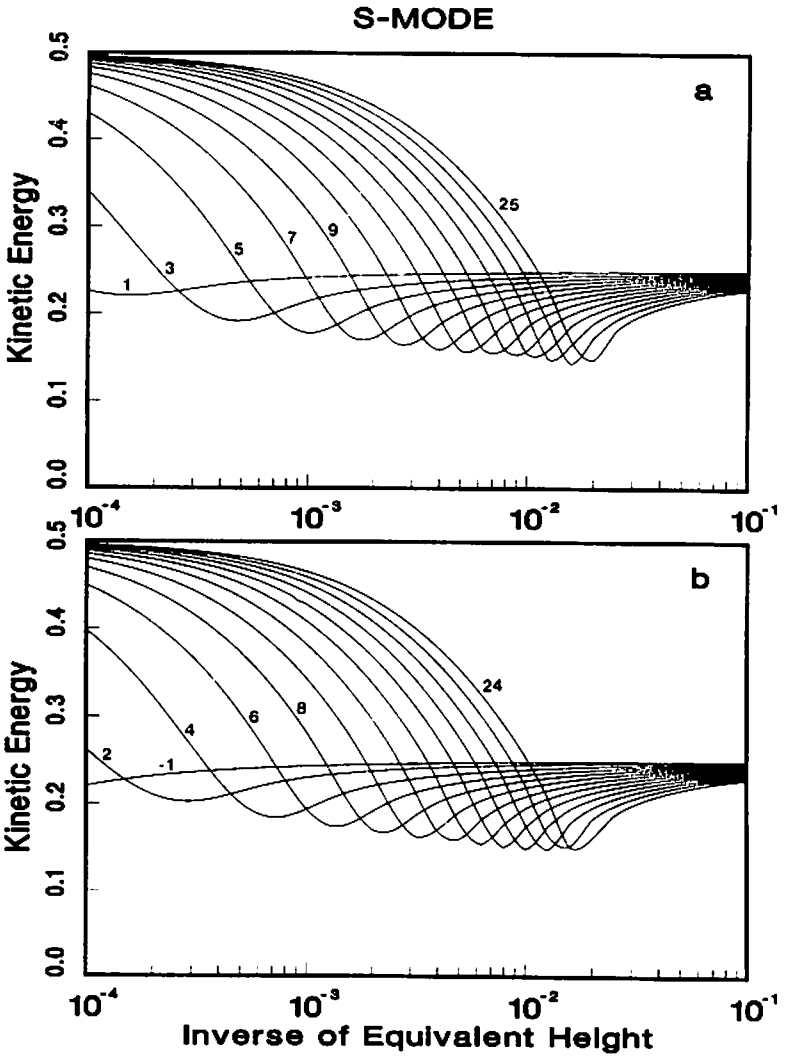

Fig. 2. As in Fig. 1, but for the S-modes. (a) Symmetric modes with odd meridional indices, and (b) antisymmetric modes with even indices. For easier distinction, the first symmetric mode $l_R = -1$ is plotted in (b) with other antisymmetric modes.

approaches zero as $h \to 0$. We see for the internal mode at $h = 10$ m that potential energy dominates over kinetic energy, i.e., Z dominates U in their variance. It can be shown from (8) that K tends to zero and P tends to 0.5 as $h \to 0$. Both symmetric and antisymmetric modes show similar characteristics. Contrasted with the antisymmetric modes, the curves of the symmetric modes twist and touch the adjacent curves in the middle of the diagram, creating a systematic intersection across the curves. This odd behavior of the symmetric modes is resulted from the application of the Gram–Schmidt procedure for orthogonalization.

The solid lines of Fig. 2 for the S-modes indicate the tendency of the energy level approaching 0.5 rapidly at $h = 10^4$ m as seen in Fig. 1. As h^{-1} increases, the energy level reduces as in the case of K-modes. However, we see clear turning points in Fig. 2 such that the K over P ratios approach to unity. It is shown by Shigehisa (1983) that both K and P tend to 0.25 as $h \to 0$. This tendency agrees with that of nonzonal rotational modes. The S-modes share common characteristics with the nonzonal rotational modes, but the K-modes do not have this feature. Particularly, the characteristics of S-modes are quite different from K-modes for small h.

3. Expansion of atmospheric data in terms of the normal mode functions

A system of three-dimensional linearized primitive equations for a compressible fluid at a resting basic state can be decomposed in a series of shallow water equations having various values of the equivalent height h_k. The quantity h_k appears as the parametric constants relating the horizontal structure functions $H_{klm}(\lambda, \theta)$ (horizontal normal modes) to the vertical structure functions $G_k(\sigma)$ (vertical normal modes). Here, $H_{klm}(\lambda, \theta)$ is the Hough harmonics in Section 2, $\sigma = p/p_b$ is a normalized pressure coordinate, and p_b is a boundary pressure (constant) near the earth's surface. The subscript m is the zonal wavenumber and l is a meridional index representing the modes of the first and second kinds in a suitable order. Note that σ here is used for the vertical coordinate, instead of the eigenfrequency. The vertical structure functions are derived from dynamical equations describing an atmospheric vertical structure, and they form a complete set of orthonormal expansion basis functions.

We represent the three-dimensional atmospheric variables of longitudinal u and meridional v wind components and geopotential deviation ϕ from a global mean reference state, as a vector $W(\lambda, \theta, \sigma) = (u, v, \phi)^T$, in terms of the following series

$$W(\lambda, \theta, \sigma) = \sum_{k,l,m} w_{klm} X_k H_{klm}(\lambda, \theta) G_k(\sigma), \qquad (15)$$

where the scaling matrix X_k is defined for each vertical index k:

$$X_k = \sqrt{gh_k}\,\mathrm{diag}(1, 1, \sqrt{gh_k}). \qquad (16)$$

The expansion coefficients w_{klm} can be determined by the use of orthonormality condition of H_{klm} and $G_k(\sigma)$. Once w_{klm} are obtained, the energy element E_{klm} in a dimensional form for a particular basis function of $m = 0$ is calculated by

$$E_{klm} = \tfrac{1}{4} p_s h_k |w_{klm}|^2 \qquad \text{for} \quad m = 0. \qquad (17)$$

In this study, we compare the energy levels for the K- and S-modes discussed in Section 2 in addition to the results of gravity modes.

The atmospheric data used are the reanalyzed GFDL FGGE IIIb data for the SOP-1. The use of the FGGE data will enable us to compare the present results with previous energetics studies (e.g., Kung 1988; Tanaka and Kung 1988). The twice daily (0000 and 1200 UTC) variables of u, v, and ϕ are given at the 12 vertical levels of 1000,

Table 1. *Vertical index k and the corresponding equivalent height h_k (m); the inverse of the equivalent height h_k^{-1} is also listed for reference*

k	h_k (m)	h_k^{-1} (m^{-1})
0	9623.9	1.0×10^{-4}
1	2297.1	4.4×10^{-4}
2	475.9	2.1×10^{-3}
3	272.0	3.7×10^{-3}
4	150.0	6.7×10^{-3}
5	79.5	1.3×10^{-2}
6	42.4	2.4×10^{-2}
7	26.3	3.8×10^{-2}
8	21.6	4.6×10^{-2}
9	13.4	7.5×10^{-2}
10	9.4	1.1×10^{-1}

850, 700, 500, 400, 300, 250, 200, 150, 100, 50, and 30 mb. The original data at 1.875° latitudinal grids are interpolated onto 60 Gaussian latitudes using cubic spline routines. The vertical structure functions $G_k(\sigma)$ for the 12 vertical levels specified above are constructed numerically according to a finite-difference scheme described by Kasahara and Puri (1981). Table 1 lists the values of the equivalent height h_k for vertical index k. The vertical mode for $k = 0$ is referred to as the external mode, whereas the rest of the vertical modes as the internal modes. Although the higher order vertical modes are sensitive to the vertical resolution, it should not cause a serious problem for the purpose of comparing K- and S-modes.

Fig. 3 illustrates the vertical energy spectra (averaged during the SOP-1) of zonal wavenumber zero as functions of h_k^{-1} for $k = 0$–10. The results exhibit the total energy, i.e., the sum of kinetic energy and available potential energy, for K- and S-modes and gravity modes. Both the positive and negative frequency gravity modes are

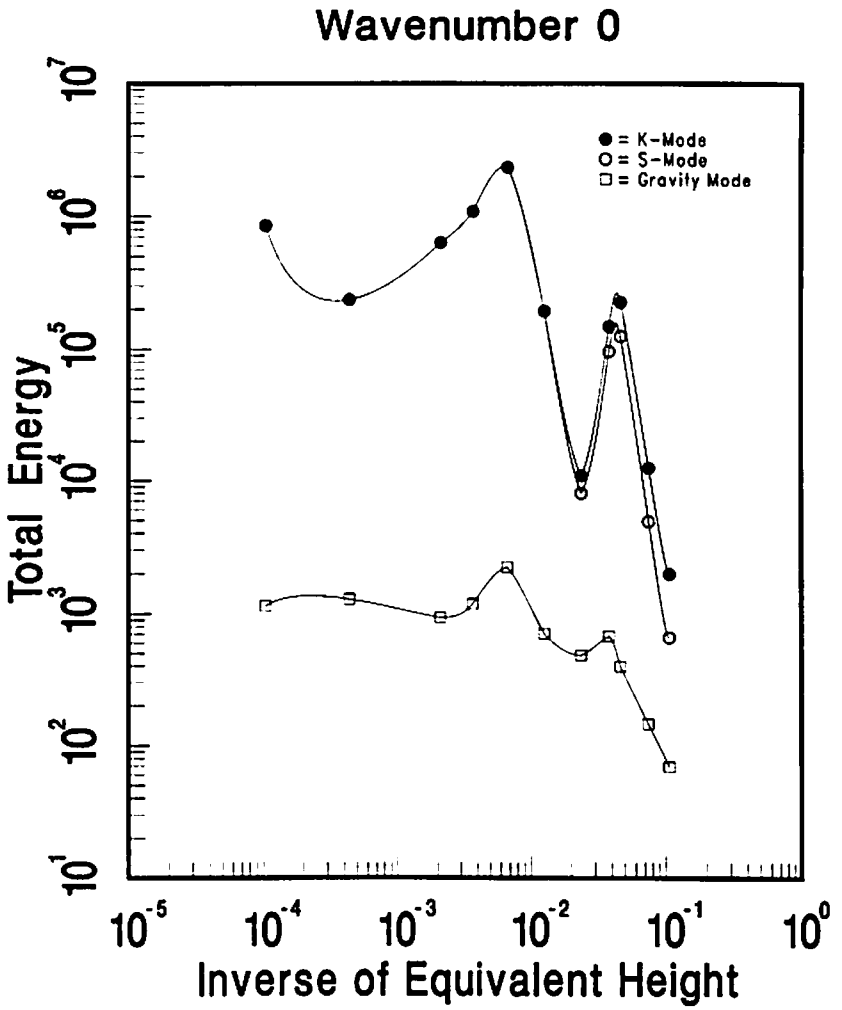

Fig. 3. Spectral distributions of atmospheric total energy of zonal wavenumber zero during the FGGE SOP-1 as functions of equivalent height h_k for $k = 0$–10. Total energy (Jm^{-2}) is the sum of kinetic energy and available potential energy. Dots denote energy projected onto the K-modes, circles denote for S-modes, and squares denote for gravity modes as the sum of positive and negative frequency modes.

used to calculate the gravity mode energy. The energy spectra are evaluated twice daily and averaged for the SOP-1. The results clearly show that the geostrophic mode energy dominates over the gravity mode energy, confirming that the geostrophic modes are essential for the expansion basis functions.

For both the K- and S-mode expansions, the energy maximum (about $23 \times 10^5\ \mathrm{Jm}^{-2}$) is seen at $h_k = 150$ m. Since the total energy for $m = 0$ is about $60 \times 10^5\ \mathrm{Jm}^{-2}$, close to one half of the energy is found near the peak at $h_k = 150$ m. The external mode at $h_k = 9624$ m contains $8.4 \times 10^5\ \mathrm{Jm}^{-2}$. Another energy peak is seen at $h_k = 22$ m. There are energy minima between $h_k = 9624$ and 150 m and between 150 and 22 m. The gravity mode energy is two orders of magnitude less than the geostrophic mode energy. Their energy peaks appear at the same h_k as seen in the geostrophic modes. Since both meridional velocity v and vertical motion ω ($= \mathrm{d}p/\mathrm{d}t$) vanish in the geostrophic modes, the meridional structure of the Hadley cell is described only by the gravity modes. Therefore, although the energy levels are low, the gravity modes are important in describing the zonal mean circulations.

The energy spectra for K- and S-modes agree well for large h_k. This suggests that the number of functions used in the K- and S-mode expansions is sufficient to represent the atmospheric data for large h_k. However, the S-mode expansion contains less energy than the K-mode expansion in small h_k. Physically speaking, the two expansion methods should yield the identical amounts of energy in each vertical mode if the number of expansion terms were infinite. Thus, the discrepancy in the amounts of energy in the S- and K-mode expansions occurs due to the difference in the ability of the expansion methods to represent the total enrgy with a finite number of expansion terms. In the following presentation, we will explain this discrepancy by examining the energy spectra of K- and S-modes for each vertical mode in the meridional index domain.

The energy spectra in the meridional index domain for the zonal wavenumber zero are illustrated in Fig. 4 for the external mode and in Fig. 5 for the internal modes. Dots denote for the K-modes, circles for S-modes, and squares for gravity modes. The four panels in Fig. 5 are for $h_k = 475$, 150, 42 and 22 m, respectively. As seen in Fig. 3, the total zonal energy is dominated by the geostrophic mode energy. Note that the $l_R = 0$ of K-modes is unique in that both U and V are identically zero and Z is a nonzero constant (see Fig. 6). Since our geopotential field is defined as the deviation from the global mean reference state, the total energy for $l_R = 0$ is identically zero; we therefore omitted the $l_R = 0$ mode. As explained in Section 2, the $l_R = -1$ mode is special in the S-modes, and $l_R = 0$ is not present. For convenience, we plotted the projected energy level of $l_R = -1$ in place of $l_R = 0$ in Figs. 4 and 5.

For the external mode ($k = 0$) in Fig. 4, these two meridional spectra of K- and S-modes are very close to each other, especially in large l_R. Nevertheless, there are minor differences in small l_R. The K-mode energy spectrum shows the maximum at $l_R = 1$, whereas the S-mode spectrum shows the maximum at $l_R = 3$. The gravity mode spectrum shows the energy maximum at $l_R = 1$.

For the internal modes ($k > 0$) in Fig. 5, the energy spectra of K- and S-modes show marked differences with respect to meridional indices. For example, as seen from Fig. 5a for the second internal mode, the energy levels of K-modes decrease almost monotonically as l_R increases starting from the maximum at $l_R = 1$, while the values of S-modes do not decrease markedly until l_R reaches 10. This means that several meridional S-modes are necessary to capture the majority of energy, while only the first two K-modes are sufficient. The tendency for the data projection onto the S-modes to require many meridional functions becomes more evident for higher internal modes. In the case of $k = 4$ ($h_k = 150$ m) on Fig. 5b, the $l_R = 1$ K-mode represents about 90% of the total energy. In contrast, energy values of S-modes increase markedly for $l_R > 7$ following an initial decrease in energy levels. The symmetric S-modes show higher energy levels than the antisymmetric S-modes for $l_R > 7$, and they appear alternately. The alternating appearance of rather large S-modes energy shifts toward a higher meridional index for higher internal modes (compare Figs. 5b through 5d.)

The different spectral distributions for the K- and S-modes are caused by notable differences in the energy characteristics of U and Z between the two sets of geostrophic modes as discussed in Section 2. In order to aid visually understanding the differences in the expansion functions, we

illustrate in Fig. 6 the meridional structures of U and Z of symmetric K- and S-modes for $h_k = 150$ m as an example of higher internal modes. Note that the differences in their structures between the K- and S-modes are substantial. The structures of the K-modes show large amplitudes of Z compared with those of U and have a global extent with large amplitudes in higher latitudes. We saw in Fig. 5b that the symmetric $l_R = 1$ K-mode represents the majority of the total energy of the $k = 4$ internal mode. This result may be explained by the fact that the structure of Z is suitable for representing the basic meridional geopotential distribution of the atmosphere, having warmer tropics and colder polar regions. In contrast, the structures of S-modes show comparable magnitudes of Z and U and have large amplitudes in low latitudes for low meridional

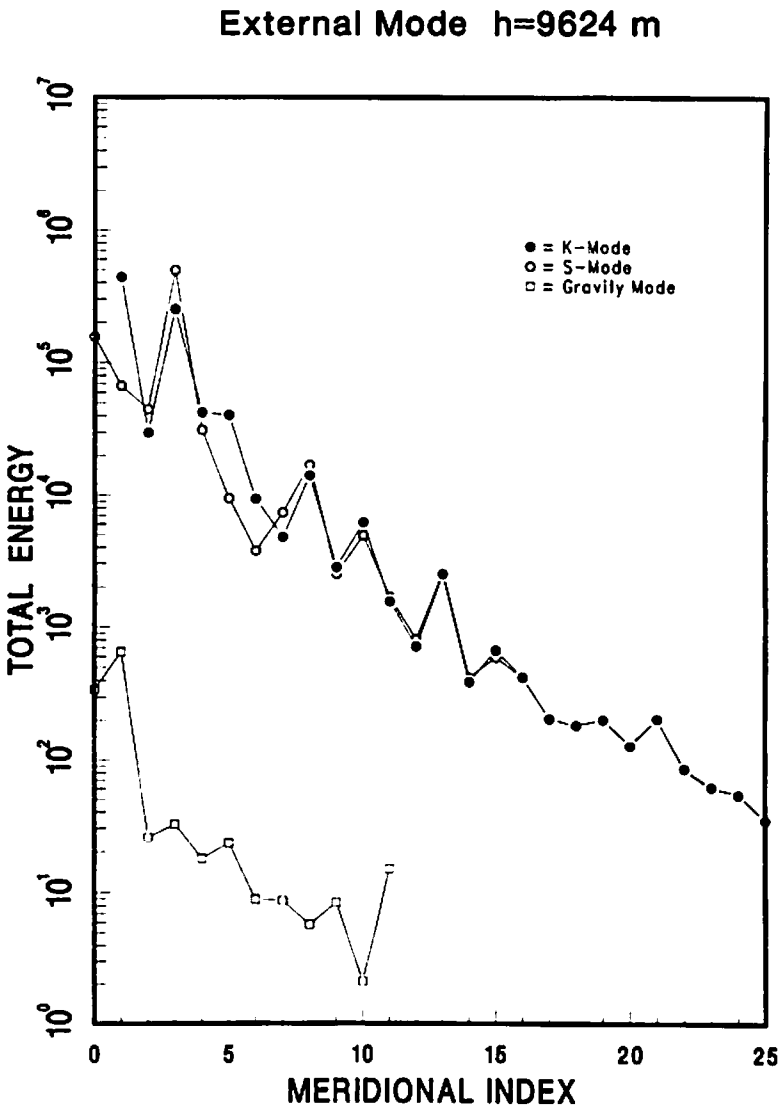

Fig. 4. Spectral distributions of atmospheric total energy of zonal wavenumber zero as functions of the meridional index l for the external mode ($k = 0$). Units are Jm^{-2}. Dots denote for the K-modes, circles for S-modes, and squares for gravity modes.

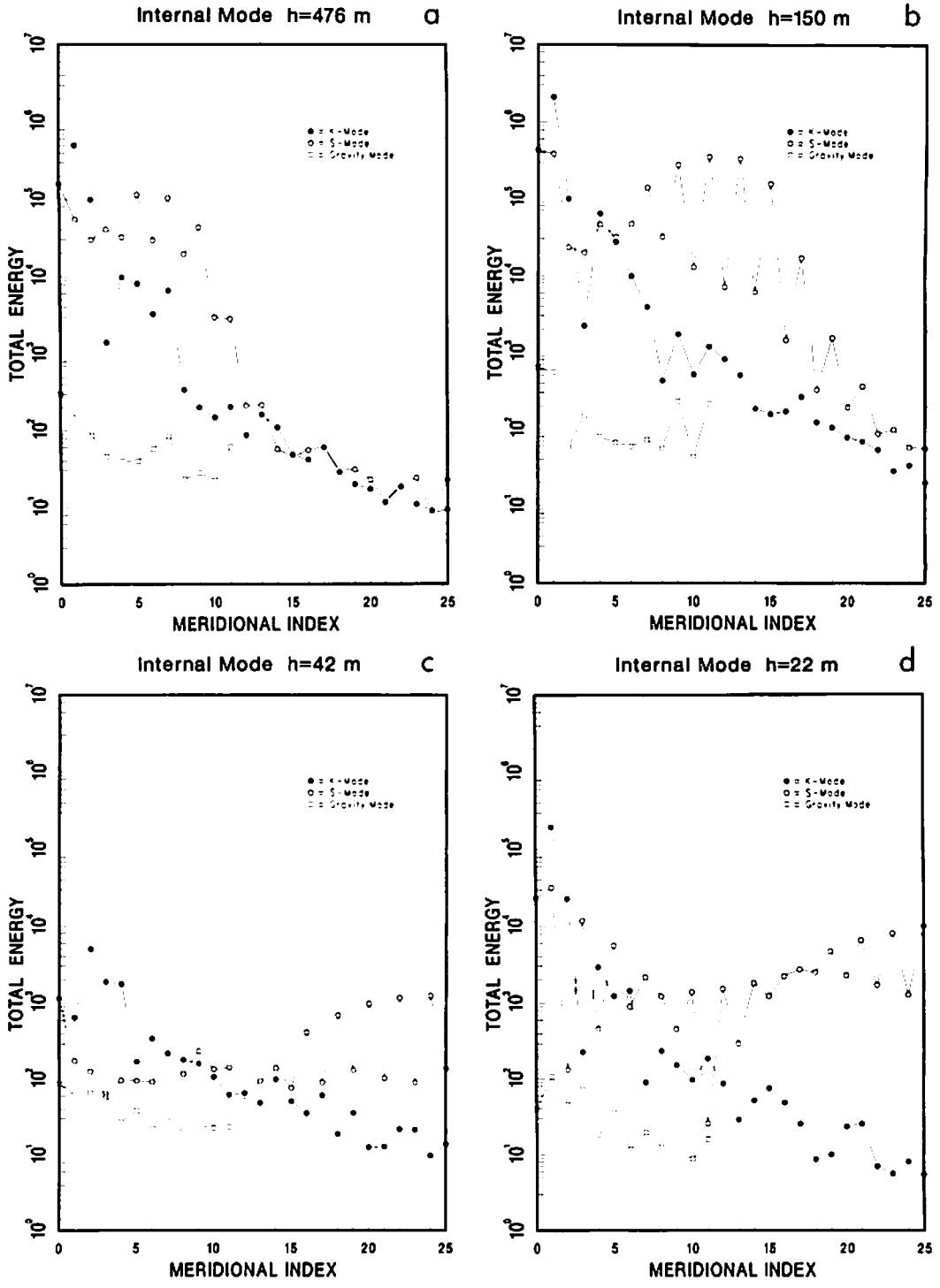

Fig. 5. As in Fig. 4, but for the internal modes ($k > 0$). The four panels (a)–(d) exhibit the energy spectra for vertical indices $k = 2$, 4, 6, and 8, respectively.

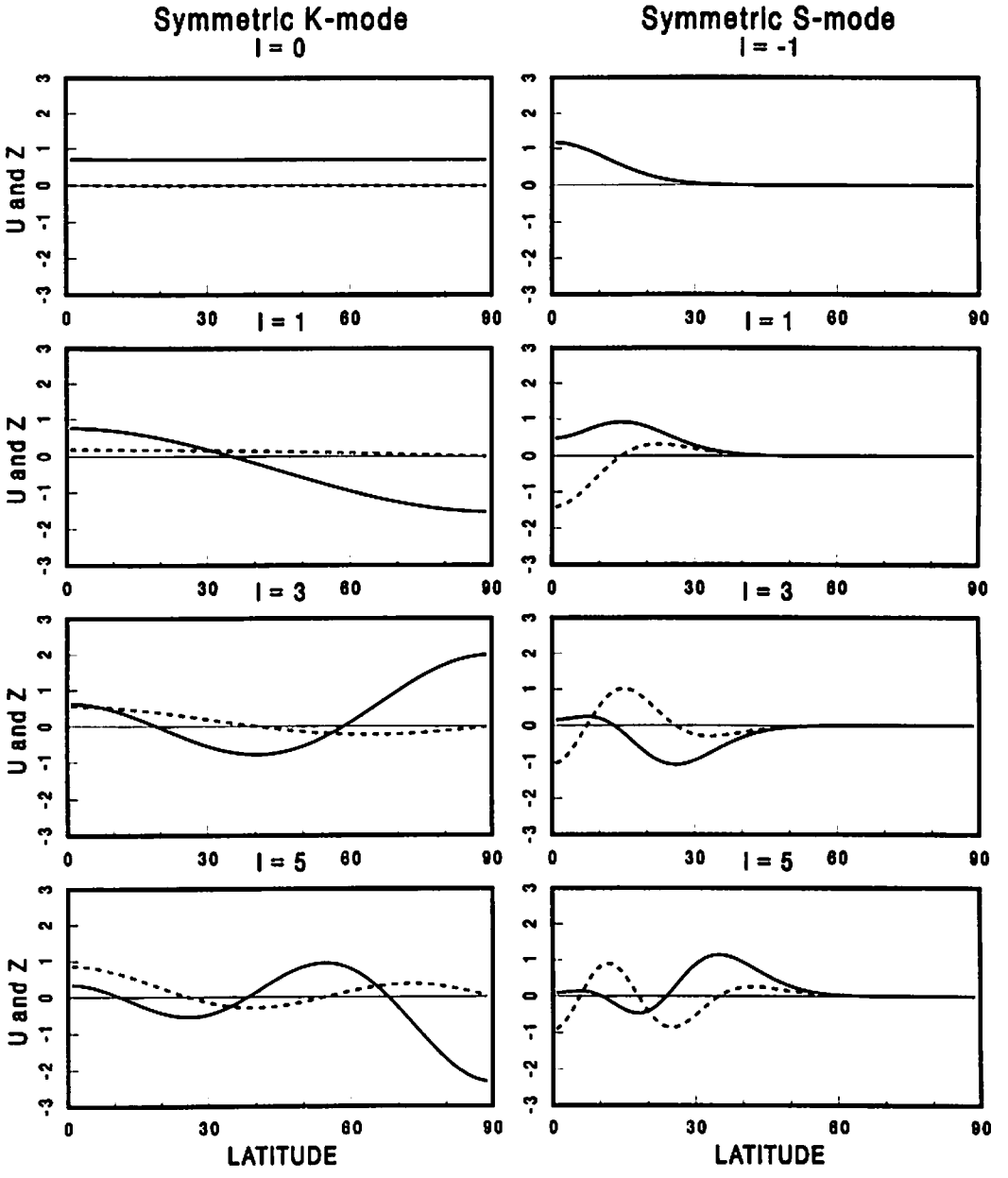

Fig. 6. Meridional structures of symmetric K-modes (left) and S-modes (right) for the internal component at $h_L = 150$ m. Solid lines denote the dimensionless geopotential Z, and dashed lines the dimensionless zonal wind U. Note that the first meridional index is $l_R = 0$ for the K-modes whereas $l_R = -1$ for the S-modes.

indices. These features resemble those of equatorially trapped internal normal modes of nonzero wavenumbers. Therefore, in order to represent higher latitude structures in terms of the S-modes it is necessary to use many terms of higher meridional indices.

Observed atmospheric zonal flows hold a large amount of available potential energy compared with kinetic energy and are nearly in geostrophic balance. Available potential energy is concentrated in a zonal internal component near $h_k = 150$ m, whereas the majority of kinetic energy is found in the zonal external component. Available potential energy dominates kinetic energy in the observed internal components (see Tanaka and Kung 1988). The K-modes have a property of large potential energy and small kinetic energy for small h_k, in addition to their globally extended structures. This property is effective in describing the distribution of atmospheric energy. The S-modes, in contrast, are suitable to represent evenly partitioned kinetic and potential energies for small h_k. We find that this partitioning is not observed in the atmosphere. The atmospheric zonal fields are fundamentally forced by differential heating. The S-modes, that have the property of free modes, are not effective to describe predominantly forced motions. Therefore, the K-mode series converge faster than the S-mode's to represent observed zonal fields. The discrepancy in energy levels between the K- and S-modes shown in Fig. 3 can be explained by the different rates of convergence with the K- and S-modes.

We pointed out that the S-modes share the properties of the rotational modes for nonzero zonal wavenumbers. This is not the case of the K-modes. The question of three-dimensional scaling at atmospheric energetics and the energy spectra associated with that scaling have been discussed, for example, by Baer (1981) and Tanaka (1985). As presented in Tanaka and Sun (1990), the normal mode energy spectra of nonzonal motions plotted against eigenfrequencies exhibit two distinct regimes with the 3 and $-\frac{5}{3}$ power laws. Although the eigenfrequency of geostrophic modes vanishes, the S-modes have finite values of c as the limit of σ/m when both σ and m approach zero. Therefore, the phase velocity c can be used as an intrinsic index, in place of the meridional scale index l_R, against which the energy spectra of S-modes are plotted. In fact, Tanaka (1985) presented the energy spectra of rotational modes plotted against the phase speed $|c| = |\sigma|/m$ for $m > 0$ and showed that the slope of the external-rotational mode energy spectra in the range of $|c| < 1.5 \times 10^{-2}$ (this dimensionless phase speed corresponds to approximately 14 m/s at the equator) follows approximately the 3-power of $|c|$. Moreover, the normal-mode energy distributions are dependent only on c and approximately independent of m. This finding may have a bearing on an interpretation of atmospheric large-scale disturbances from the standpoint of geophysical turbulence that results in stationary-transient interactions as energy transfer between different meridional scales (see Shepherd 1987).

Since the K- and S-mode expansions basically produce similar energy spectra for the external-mode motions when plotted against l_R (Fig. 4), it

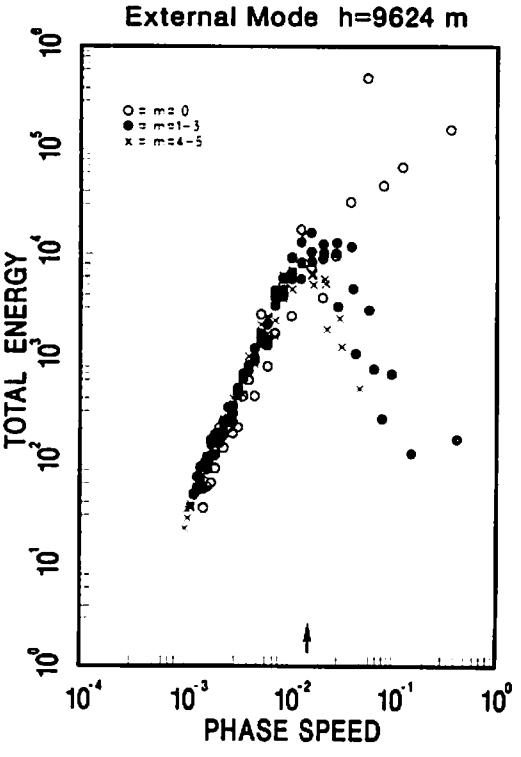

Fig. 7. Spectral distributions of atmospheric total energy of external rotational modes as functions of the dimensionless phase speed $|c|$. Units are Jm^{-2}. Circles denote for S-modes of zonal wavenumber $m = 0$, dots are for rotational modes of $m = 1 - 3$, and crosses are for those of $m = 4 - 6$.

is of interest to examine the dependence of the external-mode energy spectra on the phase speed. Fig. 7 illustrates the external-mode energy spectra for the S-modes, indicated by open circles, as a function of $|c|$. In addition, we plotted the energy spectra of the rotational disturbances for $m = 1$ to 6 by using solid dots ($m = 1$ to 3) and crosses ($m = 4$ to 6). We see clearly a 3-power range extending over $|c| < 1.5 \times 10^{-2}$. In this range, we see that the S-mode energy values fall right on other energy values for $m > 0$. The energy levels of S-modes increase for $|c| > 1.5 \times 10^{-2}$, whereas those of the nonzonal rotational modes decrease toward the $-\frac{5}{3}$ power regime (Tanaka and Sun 1990). The present result implies that the S-mode expansion is suitable to investigate the zonal atmospheric motions from the standpoint of turbulence in a similar fashion to the nonzonal atmospheric disturbances.

4. Concluding remarks

Spherical harmonics have been used extensively to represent geophysical data on the sphere. For the representation of atmospheric variables, such as the horizontal velocity components and the geopotential, an alternative is to use the normal modes of the three-dimensional primitive equations, referred to here as Hough harmonics. Advantages in the use of Hough harmonic expansion over that of spherical harmonics are that both the horizontal wind components and the geopotential are represented simultaneously with respect to a same scaling index and that it permits the identification of atmospheric motion in terms of rotational and gravity modes which has been successfully implemented in the practice of nonlinear normal mode initialization (e.g., Machenhauer 1977; Baer and Tribbia 1977). Thus, it is of interest to investigate the structure of zonal-mean atmospheric motions from the same consideration of Hough harmonic expansion for nonzonal atmospheric motions. While there is no difficulty in identifying the presence of gravity modes in zonal mean atmospheric motions, the representation of geostrophic modes has created a special problem because of the lack of appropriate expansion functions due to the fact that the eigenfrequency of geostrophic modes vanishes. To fill this need, Kasahara (1978) and Shigehisa (1983) have constructed two different sets of orthogonal eigenfunctions for the geostrophic modes. In this study, the spectral characteristics of these two different sets of geostrophic modes, which are referred to as K- and S-modes, are compared by projecting atmospheric data onto these modes. The GFDL reanalyzed FGGE IIIb data are used for this purpose. The results are summarized as follows:

Both the K- and S-modes indicate similar meridional structures of U and Z components for a large equivalent height such as $h_k = 9624$ m as pointed out by Shigehisa (1983). However, the structures of these geostrophic modes are substantially different for a smaller equivalent height. Even for a small equivalent height, the K-modes have globally extended structures, whereas the S-modes have equatorially trapped structures. The normalized kinetic energy, K ($= K_u$), and potential energy, P, of these geostrophic modes are compared for a wide range of the equivalent height. We found that $K \to 0$ and $P \to 0.5$ as $h_k \to 0$ for the K-modes. In contrast, both K and $P \to 0.25$ as $h_k \to 0$ for the S-modes.

A large portion of the atmospheric energy is stored in the zonal energy. The available potential energy dominates over the kinetic energy, and the corresponding wind and mass fields are essentially in geostrophic balance. These observations match with the characteristics of the K-modes together with the features in the energy ratio and globally extended structures. We found that the K-mode representation captures the majority of observed energy with a few meridional components, whereas the S-mode expansion requires many meridional components to express observed zonal fields satisfactorily. The S-modes exhibit some basic characteristics of free modes that are shared with the nonzonal rotational modes. The presence of observed large zonal energy associated with moderately small vertical scales in the atmosphere is resulted from forced motions due to differential heating. Therefore, the S-modes with the characteristics of free rotational motions and equatorially trapped structures for a small equivalent height are inefficient for the purpose of data expansion. The results show that the use of K-modes is superior to the S-modes in the data representation of zonal atmospheric fields due to a faster series convergence especially for internal modes. Errico (1987) adopts the K-modes for representation of

the zonal fields for normal mode initialization with the NCAR community climate model.

The eigenvalues of ϵ^{-1} associated with the S-modes may be regarded as an intrinsic index representing a kind of meridional scale of the zonal field. The observed meridional energy spectra are investigated and presented as a function of the phase speed c of the S-modes. We found that the major part of energy spectrum of the external component follows the 3 power of $|c|$. In the range of $|c| < 1.5 \times 10^{-2}$, corresponding to 14 m s at the equator, it turns out that the energy spectrum of the S-modes coincides with the energy spectra of the rotational modes for nonzonal disturbances in the external component. Moreover, the energy levels all depend only on $|c|$ and are approximately independent of the zonal wavenumber. The appearance of such a power law seems to indicate that the external zonal motions hold some characteristics of atmospheric turbulence, at least in part, generated by differential heating. This result suggests that the use of the S-mode expansion may have a potential of exploring the external zonal motions upon a different standpoint from the use of the K-mode expansion. Contrasted with this marked feature of the external energy spectrum, we find no clear trend in the dependency of energy spectra on $|c|$ for the internal components. The decision as to which geostrophic modes be used for data analysis must depend upon the nature of the investigation. For application to normal mode initialization, it is clear that the use of K-modes is advantageous, due to the faster rate of series convergence. In contrast, if the investigator is interested in the study of spectral characteristics of zonal motions in relation to those of nonzonal motions, then the use of the S-modes may be preferred.

Finally, a comment should be made concerning the effect of orography in the scale representation of atmospheric motions. In the present discussion, we formulated the normal modes and expanded with them atmospheric data on pressure surfaces, ignoring the presence of orography. Actually, the construction of normal modes and the spectral analysis can be performed based on the atmospheric system written in Phillips' sigma coordinate, as done by Kasahara and Puri (1981). Thus, effect of orography can be implicitly treated, though the definition of geopotential must be modified by an additional term representing an orographic effect. In their work, the influence of this additional term has been investigated upon the spectral analysis of atmospheric motions. They found that the observed spectral distributions in the pressure and sigma coordinates are very similar. Therefore, the use of pressure or sigma coordinates in the spectral analysis, as far as large-scale motions are concerned, will not affect our interpretation on the scale dependency of atmospheric motions in the framework of normal mode expansions. This should not be interpreted that there is no orographic effect in the atmospheric energetics. Orographic effects are reflected in the observed data and, in fact, there is no way to isolate them from the real data.

5. Acknowledgments

The authors are grateful to D. Fitzerald for reading and editing the original manuscript. This research is supported by the National Science Foundation under Grant No. ATM-8923064. Partial support has been provided through the National Oceanic and Atmospheric Administration under No. NA88AANG0140, and the National Aeronautics and Space Administration under Grant No. NAG8-809.

REFERENCES

Baer, F. 1981. Three-dimensional scaling and structure of atmospheric energetics. *J. Atmos. Sci. 38*, 52–68.

Baer, F. and Tribbia, J. J. 1977. On complete filtering of gravity modes through nonlinear initialization. *Mon. Wea. Rev. 105*, 1536–1539.

Chapman, S. and Lindzen, R. S. 1970. *Atmospheric tides*. Gordon and Breach, New York, 200 pp.

Errico, R. 1987. A Description of Software for Determination of Normal Modes of the NCAR Community Climate Model. NCAR Technical Note, NCAR/TN – 277 + STR. 86 pp.

Errico, R. 1989. Theory and application of nonlinear normal mode initialization. NCAR Technical Note, NCAR TN – 344 + IA. 145 pp.

Kasahara, A. 1976. Normal modes of ultralong waves in the atmosphere. *Mon. Wea. Rev. 104*, 669–690.

Kasahara, A. 1977. Numerical integration of the global barotropic primitive equations with Hough harmonic expansions. *J. Atmos. Sci. 34*, 687–701.

Kasahara, A. 1978. Further studies on a spectral model of the global barotropic primitive equations with Hough harmonic expansions. *J. Atmos. Sci. 35*, 2043–2051.

Kasahara, A. and Puri, K. 1981. Spectral representation of three-dimensional global data by expansion in normal mode functions. *Mon. Wea. Rev. 109*, 37–51.

Kung, E. C. 1988. Spectral energetics of the general circulation and time spectra of transient waves during the FGGE year. *J. Climate 1*, 5–19.

Longuet-Higgins, M. S. 1968. The eigenfunctions of Laplace's tidal equations over a sphere. *Phil. Trans. Roy. Soc. London A262*, 511–607.

Machenhauer, B. 1977. On the dynamics of gravity oscillations in a shallow water model with applications to nonlinear normal mode initialization. *Beiträge zur Physik der Atmosphäre 50*, 253–271.

Matsuno, T. 1966. Quasi-geostrophic motions in the equatorial area. *J. Meteor. Soc. Japan 44*, 25–43.

Salby, M. L., Garcia, R. R., O'Sullivan, D. and Tribbia, J. 1990. Global transport calculations with an equivalent barotropic system. *J. Atmos. Sci. 47*, 188–214.

Shepherd, T. G. 1987. A spectral view of nonlinear fluxes and stationary-transient interaction in the atmosphere. *J. Atmos. Sci. 44*, 1166–1178.

Shigehisa, Y. 1983. Normal modes of the shallow water equations for zonal wavenumber zero. *J. Meteor. Soc. Japan 61*, 479–493.

Silva Dias, P. L. and Schubert, W. H. 1979. The dynamics of equatorial mass-flow adjustment. Atmos. Sci. Paper No. 312, Department of Atmospheric Science, Colorado State University.

Swarztrauber, P. N. and Kasahara, A. 1985. The vector harmonics analysis of Laplace's tidal equations. *SIAM J. Sci. Stat. Comput. 6*, 464–491.

Tanaka, H. 1985. Global energetics analysis by expansion into three-dimensional normal mode functions during the FGGE winter. *J. Meteor. Soc. Japan 63*, 180–200.

Tanaka, H. L. and Kung, E. C. 1988. Normal mode energetics of the general circulation during the FGGE year. *J. Atmos. Sci. 45*, 3723–3736.

Tanaka, H. L. and Sun, S. 1990. A study of baroclinic energy source for large-scale atmospheric normal modes. *J. Atmos. Sci. 47*, 2674–2695.

Tanaka, H. L., Kung, E. C. and Baker, W. E. 1986. Energetics analysis of the observed and simulated general circulation using three-dimensional normal mode expansion. *Tellus 38A*, 412–428.

Tribbia, J. J. 1979. Nonlinear initialization on an equatorial beta-plane. *Mon. Wea. Rev. 107*, 703–713.